SPATIAL RESOLUTION PROPERTIES OF PENALIZED WEIGHTED LEAST-SQUARES TOMOGRAPHIC IMAGE RECONSTRUCTION WITH MODEL MISMATCH

Jeffrey A. Fessler

COMMUNICATIONS & SIGNAL PROCESSING LABORATORY
Department of Electrical Engineering and Computer Science
The University of Michigan
Ann Arbor, Michigan 48109-2122

Mar. 1997

Technical Report No. 308
Approved for public release; distribution unlimited.

Spatial Resolution Properties of Penalized Weighted Least-Squares Tomographic Image Reconstruction with Model Mismatch

Jeffrey A. Fessler
4240 EECS Bldg., 1301 Beal Ave., University of Michigan, Ann Arbor, MI 48109-2122
email: fessler@umich.edu, phone: 734-763-1434,
Technical Report # 308
Communications and Signal Processing Laboratory
Dept. of Electrical Engineering and Computer Science
The University of Michigan

ABSTRACT

This paper presents an analysis of the spatial resolution properties of tomographic image reconstruction based on a regularized least-squares objective function. The derivations are based on an idealized space-invariant tomographic system having a continuum of radial and angular samples. The analysis accounts for mismatch between the true radial point-spread function (PSF) of the measurements and the PSF used in the system model for image reconstruction. An angular-dependent weighting is also included, which provides insight into the asymmetric PSFs observed in images reconstructed by penalized weighted least-squares methods.

I. INTRODUCTION

All methods for tomographic image reconstruction entail tradeoffs between spatial resolution and noise. We have recently analyzed the spatial resolution [1, 2] and noise [3] properties of penalized-likelihood methods for tomographic image reconstruction. Although the discrete formulations used in [1, 2] are appropriate for computer implementation with real discrete measurements, they lack some of the insight that one can obtain from analytical methods, even though analytical results are generally based on idealized measurement systems.

This paper derives the PSF of one form of penalized least-squares tomographic image reconstruction by analyzing an idealized tomograph having a continuum of detectors and angles. The model is partially realistic, however, since we account for a radial detector blur. The analytical form we derive for this continuous tomograph shows remarkable agreement with simulations using discrete sampled systems.

This work was supported in part by the Whitaker Foundation and NIH grants CA-60711 and CA-54362.

II. THEORY: PSF OF IDEALIZED TOMOGRAPH

A. Notation

Let $f(x_1, x_2)$ denote an object intensity function defined over $\mathbb{R}^2$. Let $\mathcal{P}$ denote the continuous Radon transform operator. If $p = \mathcal{P}f$, then

$$\begin{aligned} p_\phi(r) &= \int f(l\cos\phi + r\sin\phi,\ l\sin\phi - r\cos\phi)\, dl \\ &= \iint f(x_1, x_2)\delta(x_1\cos\phi + x_2\sin\phi - r)\, dx_1\, dx_2. \end{aligned}$$

Define the following inner product for "sinogram space:"

$$\langle q, p\rangle = \int_0^\pi \int_{-\infty}^\infty q_\phi^\star(r) p_\phi(r)\, dr\, d\phi,$$

and associated norm $\|p\|^2 = \langle p, p\rangle$. The adjoint of $\mathcal{P}$ under the above inner product is the backprojection operator $\mathcal{B}$, i.e. $\mathcal{P}' = \mathcal{B}$. If $b = \mathcal{B}p$ then

$$b(x_1, x_2) = \int_0^\pi p_\phi(x_1\cos\phi + x_2\sin\phi)\, d\phi.$$

Proof: if $p = \mathcal{P}f$ then

$$\begin{aligned} \langle q, \mathcal{P}f\rangle &= \int_0^\pi \int_{-\infty}^\infty q_\phi^\star(r) p_\phi(r)\, dr\, d\phi \\ &= \int_0^\pi \int_{-\infty}^\infty q_\phi^\star(r) \iint f(x_1, x_2) \cdot \\ &\qquad \delta(x_1\cos\phi + x_2\sin\phi - r)\, dx_1\, dx_2\, dr\, d\phi \\ &= \iint f(x_1, x_2) \cdot \end{aligned}$$

$$\begin{aligned} & \int_0^\pi q_\phi^\star(x_1 \cos\phi + x_2 \sin\phi)\, d\phi\, dx_1\, dx_2 \\ = & \iint f(x_1,x_2)\, (\mathcal{B}q)^\star(x_1,x_2)\, dx_1\, dx_2 \\ = & \langle \mathcal{B}q, f \rangle, \end{aligned}$$

where the image-space inner product is the standard choice for $L_2(\mathbb{R}^2)$. (We assume sufficient regularity conditions to enable any necessary changes of order of integration.)

Let $\mathcal{S}_{\mathrm{true}}$ denote a space-invariant *radial* sinogram blurring operator with symmetric kernel $s_{\mathrm{true}}(r)$. If $y = \mathcal{S}_{\mathrm{true}} p$, then

$$y_\phi(r) = s_{\mathrm{true}}(r) * p_\phi(r),$$

where $*$ denotes 1D convolution.

Define $\mathcal{G}_{\mathrm{true}} = \mathcal{S}_{\mathrm{true}}\mathcal{P}$ to be the blurred Radon transform operator. The operator $\mathcal{G}_{\mathrm{true}}$ is the continuous analog of the system matrix $\boldsymbol{G}$ in [1]. Given measurements with additive zero-mean noise:

$$y = \mathcal{G}_{\mathrm{true}} f + \text{noise},$$

we would like to recover f from y.

B. Reconstruction

We may not know the blur function $\mathcal{S}_{\mathrm{true}}$ exactly, but rather may only have an approximation $\mathcal{S}_{\mathrm{model}}$ with kernel $s_{\mathrm{model}}(r)$. A penalized least squares (PLS) approach to this problem is:

$$\hat{f} = \arg\min_f \|y - \mathcal{G}_{\mathrm{model}} f\|_{\mathcal{W}}^2 + \alpha \langle f, \mathcal{R} f \rangle, \qquad (1)$$

where $\mathcal{G}_{\mathrm{model}} = \mathcal{S}_{\mathrm{model}}\mathcal{P}$, and the weighted norm is defined by $\|p\|_{\mathcal{W}}^2 = \langle p, \mathcal{W}p \rangle = \langle \mathcal{W}p, p \rangle$ where if $q = \mathcal{W}p$ then $q_\phi(r) = w_\phi(r) p_\phi(r)$. The weights $w_\phi(r)$ must be real, i.e. $w_\phi^\star(r) = w_\phi(r)$, and positive. The operator $\mathcal{W}$ is the continuous analog of the diagonal matrix $\mathrm{diag}\{u_i\}$ in [1].

If we desire smooth solutions $\hat{f}$, then we would like $\langle f, \mathcal{R} f \rangle$ to be a measure of roughness. Therefore we define $\mathcal{D}_j$ to be the differentiation operator with respect to the jth spatial coordinate:

$$(\mathcal{D}_j f)(x_1,x_2) = \frac{\partial}{\partial x_j} f(x_1,x_2), \quad j = 1,2.$$

Thus

$$\|\mathcal{D}_j f\|^2 = \iint \left(\frac{\partial}{\partial x_j} f(x_1,x_2) \right)^2 dx_1\, dx_2.$$

By defining

$$\mathcal{R} = (\mathcal{D}_1'\mathcal{D}_1 + \mathcal{D}_2'\mathcal{D}_2)^m, \qquad (2)$$

we have specified $\langle f, \mathcal{R} f \rangle$ to be an isotropic measure of the roughness of f. (Note that operators $\mathcal{D}_1$ and $\mathcal{D}_2$ commute.) In particular, for the usual choice $m = 1$, we have

$$\mathcal{R} = \mathcal{D}_1'\mathcal{D}_1 + \mathcal{D}_2'\mathcal{D}_2,$$

which is analogous to the matrix $\boldsymbol{R}^\star$ (for the quadratic penalty) in [1].

Assuming $s_{\mathrm{model}}(r)$ is a low-pass filter whose transfer function $S_{\mathrm{model}}(u)$ is nonzero at $u = 0$, one can easily show that the null spaces of $\mathcal{G}_{\mathrm{model}}$ and $\mathcal{R}$ are disjoint, so the solution to (1) is

$$\hat{f} = [\mathcal{G}_{\mathrm{model}}'\mathcal{W}\mathcal{G}_{\mathrm{model}} + \alpha\mathcal{R}]^{-1}\mathcal{G}_{\mathrm{model}}'\mathcal{W}y,$$

and the estimator mean is:

$$\begin{aligned} \mu(f) &= E\{\hat{f}\} \\ &= [\mathcal{G}_{\mathrm{model}}'\mathcal{W}\mathcal{G}_{\mathrm{model}} + \alpha\mathcal{R}]^{-1}\mathcal{G}_{\mathrm{model}}'\mathcal{W}\mathcal{G}_{\mathrm{true}} f \qquad (3) \end{aligned}$$

If $\mathcal{W}$ is the identity operator, then (3) represents a space-invariant mean response, i.e. $\mu(f)$ corresponds to a filtered version of f. We now use Fourier methods to derive the frequency response of that filter.

C. Frequency Response

It is well known [4] that

$$\mathcal{P}'\mathcal{P} f = \frac{1}{r} ** f,$$

where $**$ denotes 2D convolution. If we let u_1 and u_2 denote the 2D spatial frequency coordinates, and define $\rho = \sqrt{u_1^2 + u_2^2}$, then since the 2D Fourier transform of $1/r$ is $1/\rho$, we have

$$\mathcal{P}'\mathcal{P} = \mathcal{F}_2' \cdot \frac{1}{\rho} \cdot \mathcal{F}_2,$$

where $\mathcal{F}_2$ denotes the 2D Fourier operator. (We use the orthonormal version of $\mathcal{F}_2$, i.e., scaled so that $\mathcal{F}_2'\mathcal{F}_2$ is the identity operator.)

However, we would like to express $\mathcal{P}'\mathcal{W}\mathcal{P}$ in the Fourier domain, not just $\mathcal{P}'\mathcal{P}$. This is probably not possible for an arbitrary operator $\mathcal{W}$. Delaney and Bresler consider spectral operators $\mathcal{W}$ to derive a preconditioner [5]. Here, we restrict attention to weighting functions that are radially invariant, i.e. $w_\phi(r) = w_\phi$ is independent of radial position r. In this case one can use the Fourier-slice theorem to show that

$$\mathcal{P}'\mathcal{W}\mathcal{P} = \mathcal{F}_2' \cdot \frac{w_\phi}{\rho} \cdot \mathcal{F}_2, \qquad (4)$$

Since the blur operator $\mathcal{S}_{\text{model}}$ acts radially, by the Fourier-slice theorem:

$$\mathcal{G}'_{\text{model}} \mathcal{W} \mathcal{G}_{\text{model}} = \mathcal{F}'_2 \cdot \frac{w_\phi |S_{\text{model}}(\rho)|^2}{\rho} \cdot \mathcal{F}_2. \quad (5)$$

Similarly

$$\mathcal{G}'_{\text{model}} \mathcal{W} \mathcal{G}_{\text{true}} = \mathcal{F}'_2 \cdot \frac{w_\phi S^\star_{\text{model}}(\rho) S_{\text{true}}(\rho)}{\rho} \cdot \mathcal{F}_2.$$

One can express the differentiation property of Fourier transforms [6] as $\mathcal{D}_j = \mathcal{F}'_2 (i 2\pi u_j) \mathcal{F}_2$ where $i = \sqrt{-1}$. Therefore we have:

$$\mathcal{D}'_j \mathcal{D}_j = \mathcal{F}'_2 \cdot (2\pi u_j)^2 \cdot \mathcal{F}_2,$$

so

$$\begin{aligned} \mathcal{R} &= (\mathcal{D}'_1 \mathcal{D}_1 + \mathcal{D}'_2 \mathcal{D}_2)^m \\ &= \mathcal{F}'_2 \cdot [(2\pi u_1)^2 + (2\pi u_2)^2]^m \cdot \mathcal{F}_2 \\ &= \mathcal{F}'_2 \cdot (2\pi\rho)^{2m} \cdot \mathcal{F}_2. \end{aligned} \quad (6)$$

(This confirms the statement following (2) that (2) yields an isotropic measure of roughness.)

Combining (3), (5), and (6) shows that

$$\mu(f) = \mathcal{F}'_2 \cdot L_0(\rho, \phi) \cdot \mathcal{F}_2 f,$$

where the frequency response $L_0(\rho, \phi)$ of the PLS estimator is therefore:

$$\begin{aligned} L_0(\rho,\phi) &= \frac{\underline{\frac{w_\phi S^\star_{\text{model}}(\rho) S_{\text{true}}(\rho)}{\rho}}}{\frac{w_\phi |S_{\text{model}}(\rho)|^2}{\rho} + \alpha (2\pi\rho)^{2m}} \\ &= \boxed{\frac{w_\phi S^\star_{\text{model}}(\rho) S_{\text{true}}(\rho)}{w_\phi |S_{\text{model}}(\rho)|^2 + \beta_0 \rho^{2m+1}},} \end{aligned} \quad (7)$$

where $\beta_0 = \alpha (2\pi)^{2m}$.

Note that if w_ϕ is a constant, then the frequency response is radially-symmetric. Otherwise the frequency response, and hence the point-spread function, will be asymmetric if the conventional radially-symmetric regularization method (2) is used, as observed in [1]. However, in principle we can eliminate this asymmetry by applying a regularization operator whose frequency response is proportional to w_ϕ (times any power of ρ). In practice, for a discrete implementation of the regularization operator the asymmetry should be approximately eliminated.

Note that the frequency response (7) is nonnegative function. Therefore it is somewhat unsurprising that negative sidelobes are often observed in the PSFs.

Not surprisingly, the frequency response (7) is unity near $\rho = 0$, and then typically decreases with increasing spatial frequency. The form of (7) is very similar to a constrained least-squares restoration filter [7], or for an ideal system with $S_{\text{model}}(u) = S_{\text{true}}(u) = 1$, to a Butterworth low-pass filter. Typical plots of $L_0(\rho)$ are shown in Figs. 1-4 for the case $w_\phi = 1$, which we assume hereafter unless otherwise stated.

D. Point Spread Function

Since the frequency response is radially symmetric for $w_\phi = 1$, one can compute the corresponding PSF $l_0(r)$ using the Hankel transform [6]:

$$l_0(r) = 2\pi \int_0^\infty L_0(\rho)\ J_0(2\pi\rho r)\ \rho\, d\rho, \quad (8)$$

where J_0 is the 0th order Bessel function. We do not know of an analytical form for the Hankel transform of (7), even when $S_{\text{true}}(u) = S_{\text{model}}(u) = 1$, but it is easy to evaluate the integral numerically. As $\beta_0 \to 0$, the FWHM of $l_0(r)$ approaches 0, whereas for a discrete system, the smallest possible FWHM is 1 pixel. Therefore, we also define the blurred response:

$$l_1(r) = l_0(r) * 1_{\{|r| \le 1/2\}}, \quad (9)$$

where $1_{\{|r| \le 1/2\}}$ denotes the standard rectangular function. As $\beta_0 \to 0$, the FWHM of $l_1(r)$ approaches 1, which better agrees with the discrete results.

Typical plots of the normalized PSF $l_0(r)/l_0(0)$ are shown in Figs. 5-8, for several values of β_0 and for different radial blurs $S_{\text{true}}(u) = S_{\text{model}}(u)$ with no model mismatch. Note that when β_0 is small, the point response functions exhibit ringing.

By computing $l_1(r)$ using a very fine discretization of (8) and (9), we can tabulate the relationship between β_0 and the FWHM of the PSF. Typical curves are shown in Fig. 9, for different $S_{\text{true}}(u) = S_{\text{model}}(u)$ cases. In principle, one can choose a desired resolution, and then read off the appropriate β_0 from Fig. 9. This value of β_0 will be proportional to the value of β that should be used with the modified penalty of [1]. The proportionality constant is object independent, so only needs to be determined once for a given geometric system matrix $\boldsymbol{G}$ as described in [1]. The constant depends on the units one uses when defining $\boldsymbol{G}$ and the matrix $\boldsymbol{R}^\star$ of [1]. For a strip-integral tomographic system $\boldsymbol{G}$, we normalize the elements of $\boldsymbol{G}$ so that $\sum_i g_{ij} = 1$, which is "count preserving." In this case, careful bookkeeping showed that

$$\beta_0 = \beta \frac{4\pi^4}{\Delta_\theta \Delta_b}, \quad (10)$$

where Δ_θ is the angular spacing and Δ_b is the radial center-to-center spacing of the strip integrals.

Using this relationship between β and β_0, we computed the *discrete* local impulse response using (38) of [1] and the corresponding *analytical* impulse response (9) and plotted the FWHM of the two in Fig. 10, for the case of a rectangular radial blur with FWHM=2 pixels, i.e. $S_{\mathrm{true}}(u) = S_{\mathrm{model}}(u) = \mathrm{sinc}(() 2u)$. For resolutions greater than about 2 pixels FWHM, the resolution of the discrete and analytical impulse responses agree quite well. (For FWHM below 2 pixels, the effects of the discrete pixels apparently yield a slightly greater FWHM than predicted by (9).) Figure 11 displays the analytical PSF (9) and the discrete local impulse response (38) of [1] for the case $\beta_0 = 175$, for a tomograph with rectangular strip integrals with two pixel width. The agreement shown in Figs. 10 and 11 confirms that one can use Fig. 9 in conjunction with relationship like (10) to determine a value for β that will provide reconstructed images having the user's desired spatial resolution.

We remind the reader that the fact that this PLS estimator gives a response similar to a Butterworth filter does not imply that in general penalized-likelihood estimation is equivalent to Butterworth filtering! The above analysis does not include nonnegativity, Poisson statistics, realistic system modeling, nonquadratic penalties, and the other well-known advantages of statistical methods. However, the above analysis is useful for understanding and quantifying basic resolution properties. It is also useful for designing preconditioners for fast gradient-based iterative methods [8, 9].

E. A FWHM Rule of Thumb

It is well known that the FWHM of bump-shaped point spread functions is approximately equal to $1/(2\rho_h)$, where ρ_h is the half-amplitude frequency, i.e. $L_0(\rho_h) = \frac{1}{2} L_0(0)$. From (7), it is clear that the half-amplitude frequency for the PLS estimator is $\beta_0^{-1/(2m+1)}$ for the ideal case when $S_{\mathrm{true}}(u) = 1$. Thus for the usual $m = 1$ case, the FWHM of $l_0(r)$ is approximately $\beta_0^{1/3}$. Since we are more interested in $l_1(r)$, Fig. 15 displays the FWHM of $l_1(r)$ versus $\beta_0^{1/3}$ for various detector blurs. There is a nearly affine relationship between the FWHM of $l_1(r)$ and $\beta_0^{1/3}$ for $\beta_0 > 5$, which may be used to simplify further the table lookup method for relating β to FWHM described in [1].

III. LS Design of Penalty

To yield uniform spatial resolution, we would like a penalty function whose spectrum is $w_\phi \rho^n$, where n is a free design choice. To match the spatial resolution properties of unweighted penalized least squares, the target spectrum is $w_\phi \rho^{2m}$, *i.e.* $n = 2m$. The usual choice is $m = 1$, *i.e.* $n = 2$. This section describes a practical approach to designing such a penalty function.

In a discrete implementation, we cannot produce penalty functions with arbitrary angular variations. However, we can produce penalty functions whose spectrum is approximately

$$R(\rho, \phi; \underline{r}) = \sum_{k=1}^{K} r_k \rho^n \cos^n \left(\phi - \pi \frac{k-1}{K} \right).$$

For example, the $k = 1$ term is just $\rho^n \cos^n \phi = u_1^n$, which corresponds to a penalty in the x_1 direction, and the $k = K/2 + 1$ term is just $\rho^n \cos^n(\phi - \pi/2) = \rho^n \sin^n \phi = u_2^n$, which corresponds to a penalty in the x_2 direction.

Now we can attempt a (weighted) least-squares fit of the filter coefficients $\underline{r} = [r_1, \ldots, r_K]$ to make $R(\rho, \phi)$ "best" approximate $w_\phi \rho^n$. Objective function:

$$\Phi(\underline{r}) = \int_0^\pi \int_0^\infty \omega(\rho) \left[R(\rho, \phi; \underline{r}) - w_\phi \rho^n \right]^2 \, d\rho d\phi$$

where $\omega(\rho)$ is some arbitrary nonnegative weighting function. Simplifying, we find that

$$\Phi(\underline{r}) \propto \int_0^\pi \left[\sum_{k=1}^{K} r_k \cos^n \left(\phi - \pi \frac{k-1}{K} \right) - w_\phi \right]^2 \, d\phi,$$

so the ρ weighting function is irrelevant. Minimizing $\Phi(\underline{r})$ is a linear least-squares problem that is equivalent to solving the linear system of equations

$$\boldsymbol{\Phi} \underline{r} = \underline{b}$$

where

$$b_k = \frac{1}{\pi} \int_0^\pi w_\phi \cos^n \left(\phi - \pi \frac{k-1}{K} \right) d\phi \qquad (11)$$

and

$$\boldsymbol{\Phi}_{jk} = \frac{1}{\pi} \int_0^\pi \cos^n \left(\phi - \pi \frac{j-1}{K} \right) \cos^n \left(\phi - \pi \frac{k-1}{K} \right) d\phi.$$

I suspect there is an analytical inverse for $\boldsymbol{A}$. Certainly there is in the $K = 2$ case.

For discrete w_ϕ we can replace the integral in (11) with a sum, so $\underline{r} = \boldsymbol{\Phi}^{-1} \underline{b} = \boldsymbol{\Phi}^{-1} \boldsymbol{B} \underline{w}$ where $\boldsymbol{B}$ is a simple $\dim(\underline{r}) \times n_\phi$ matrix.

Simplest in the case $n = 2$, which is probably all we need.

Unfortunately, for $n > 3$ $\mathbf{\Phi}$ will be singular for $n = 2$, as noted by Web Stayman. A practical approach therefore is just to discretize the objective function rather than the solution:

$$\Phi(\underline{r}) = \sum_j \omega_j \sum_k \left[R(\rho_j, \phi_k; \underline{r}) - w_{\phi_k} \rho_j^n \right]^2 .$$

This is a simple linear least-squares problem in $\underline{r}$. However, now the ρ weighting is relevant, and must be considered.

IV. FFT Simplifications

If the geometric system response $\boldsymbol{G}$ is approximately space invariant, and if the target penalty $\boldsymbol{R}^\star$ is the standard quadratic penalty, then if one uses the modified quadratic penalty of [1], then the local impulse response is approximately given by (38) of [1]. In this important case, one can use FFT's to compute (38) of [1] approximately, thereby eliminating the need for an iterative method to compute (38) of [1].

Let j denote the index of a pixel near the center of the image, and compute the kernel $k_{G'G} = \boldsymbol{G}'\boldsymbol{G}\underline{e}^j$. Let k_R be the kernel of $\boldsymbol{R}$: $k_R = \boldsymbol{R}\underline{e}^j$. Let $f_{G'G}(u_1, u_2)$, $f_R(u_1, u_2)$, and $F_{\mathrm{UPLS}}(u_1, u_2)$ denote the 2D FFT's of $k_{G'G}$, k_R, and $[\boldsymbol{G}'\boldsymbol{G} + \beta\boldsymbol{R}^\star]^{-1}\boldsymbol{G}'\boldsymbol{G}\underline{e}^j$ respectively.

For the standard second-order quadratic penalty, the kernel of the regularization matrix $\boldsymbol{R}^\star$ is

$$\begin{bmatrix} 0 & -1 & 0 \\ -1 & 4 & -1 \\ 0 & -1 & 0 \end{bmatrix} + \frac{1}{\sqrt{2}} \begin{bmatrix} -1 & 0 & -1 \\ 0 & 4 & 0 \\ -1 & 0 & -1 \end{bmatrix} . \qquad (12)$$

Then from standard properties of circulant matrices [10]:

$$F_{\mathrm{UPLS}}(u_1, u_2) = \frac{f_{G'G}(u_1, u_2)}{f_{G'G}(u_1, u_2) + \alpha f_R(u_1, u_2)} .$$

Thus one can compute (38) of [1] using two 2D FFT's and one 2D inverse FFT.

For systems where the geometric response can be factored into product of the discretized Radon transform with a space-invariant blur, one can further simplify the calculation above.

One useful approximation to the kernel of $\boldsymbol{G}'\boldsymbol{G}$ is

$$f(r) = \begin{cases} \pi - 2r, & r \in [0, 1] \\ 2(\arcsin(1/r) - (r - \sqrt{r^2 - 1})) & r > 1, \end{cases} ,$$

which is shown in Figure 2 of [11] (cf [12, Fig. 11] and [8, Fig. 1]). This function has the expected $1/r$ asymptotic form, but is well behaved near zero—as it must be for a discrete system.

V. Discussion

We have analyzed the frequency response and point-spread function of a continuous idealized method for tomographic image reconstruction using a penalized least squares criterion. The analysis includes the effects of mismatch in the detector blur. The effects of an angularly-dependent weighting were shown to yield an asymmetric point-spread function; such asymmetries were reported in [1]. It appears that it may be possible to develop a new modified penalty function that eliminates this asymmetry by incorporating a corresponding angular dependence into the regularizer.

For data with Poisson noise, the effective angular weighting will be different for each pixel, but should vary slowly with spatial location.

References

[1] J. A. Fessler and W. L. Rogers. Spatial resolution properties of penalized-likelihood image reconstruction methods: Space-invariant tomographs. *IEEE Tr. Im. Proc.*, 5(9):1346–58, September 1996.

[2] J. A. Fessler. Resolution properties of regularized image reconstruction methods. Technical Report 297, Comm. and Sign. Proc. Lab., Dept. of EECS, Univ. of Michigan, Ann Arbor, MI, 48109-2122, August 1995.

[3] J. A. Fessler. Mean and variance of implicitly defined biased estimators (such as penalized maximum likelihood): Applications to tomography. *IEEE Tr. Im. Proc.*, 5(3):493–506, March 1996.

[4] A. C. Kak and M. Slaney. *Principles of computerized tomographic imaging*. IEEE Press, New York, 1988.

[5] A. H. Delaney and Y. Bresler. A fast and accurate Fourier algorithm for iterative parallel-beam tomography. *IEEE Tr. Im. Proc.*, 5(5):740–53, May 1996.

[6] R. Bracewell. *The Fourier transform and its applications*. McGraw-Hill, New York, 1978.

[7] B. C. Penney, M. A. King, and R. B. Schwinger. Constrained least-squares restoration of nuclear medicine images: selecting the coarseness function. *Med. Phys.*, 14(5):849–58, September 1987.

[8] N. H. Clinthorne, T. S. Pan, P. C. Chiao, W. L. Rogers, and J. A. Stamos. Preconditioning methods for improved convergence rates in iterative reconstructions. *IEEE Tr. Med. Im.*, 12(1):78–83, March 1993.

[9] S. D. Booth and J. A. Fessler. Combined diagonal/Fourier preconditioning methods for image reconstruction in emission tomography. In *Proc. IEEE Intl. Conf. on Image Processing*, volume 2, pages 441–4, 1995.

[10] A. K. Jain. *Fundamentals of digital image processing*. Prentice-Hall, New Jersey, 1989.

[11] J. A. Fessler. Penalized weighted least-squares image reconstruction for positron emission tomography. *IEEE Tr. Med. Im.*, 13(2):290–300, June 1994.

[12] K. Sauer and C. Bouman. A local update strategy for iterative reconstruction from projections. *IEEE Tr. Sig. Proc.*, 41(2):534–48, February 1993.

The author's preprints are available on the WWW from URL `http://www.eecs.umich.edu/~fessler`.

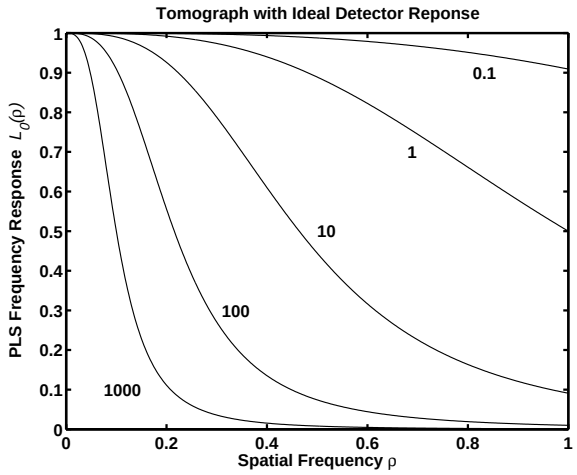

Figure 1: Plots of $L_0(\rho)$, the spatial frequency response of penalized least squares, under the continuous model described in Section II, for several values (shown) of the regularization parameter β_0, for the ideal tomograph with $S_{\rm true}(u) = 1$.

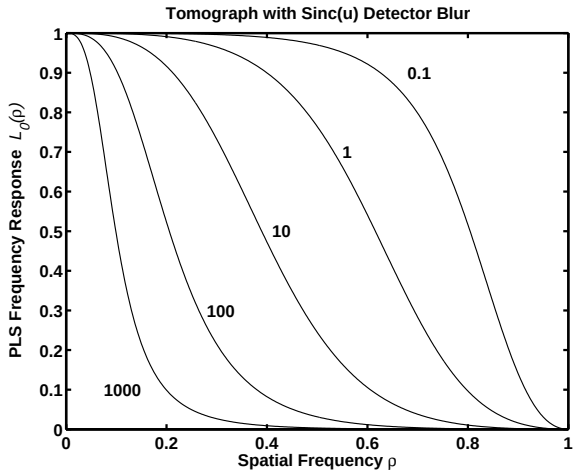

Figure 2: As in Fig. 1, but for a tomograph with a rectangular detector blur: $S_{\rm true}(u) = \mathrm{sinc}(u)$.

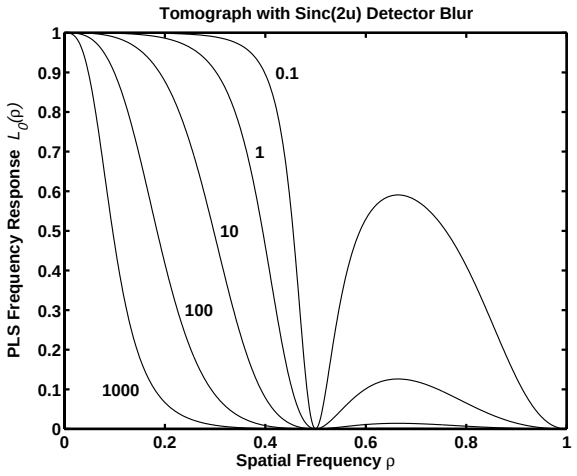

Figure 3: As in the previous figure, except $S_{\rm true}(u) = \mathrm{sinc}(2u)$.

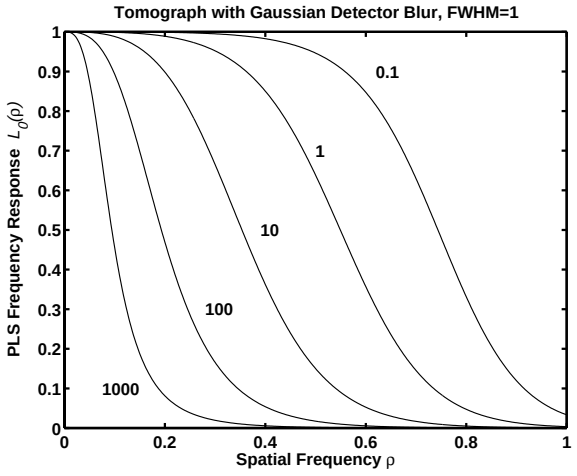

Figure 4: As in Fig. 1, but for a tomograph with a Gaussian detector blur: $S_{\rm true}(u) = \exp(-2\pi^2 u^2/\sigma^2)$, where $\sigma = (8 \log 2)^{-1/2}$ so that the FWHM of $s_{\rm true}(r)$ is approximately 1.

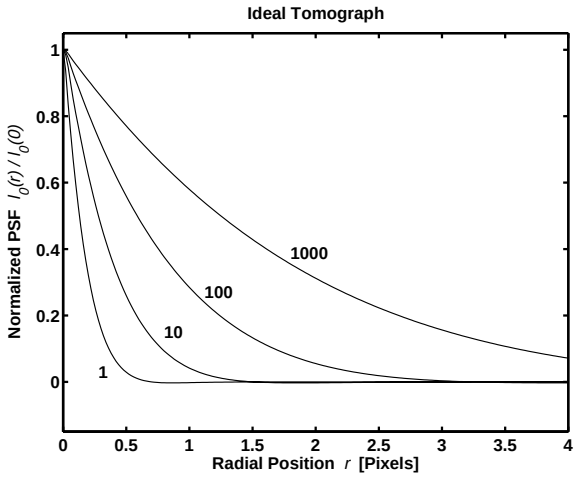

Figure 5: Plots of $l_0(r)/l_0(0)$, the impulse response or PSF of penalized least squares, under the continuous model described in Section II, for several values (shown) of the regularization parameter β_0, for the ideal case $S_{\rm true}(u) = 1$.

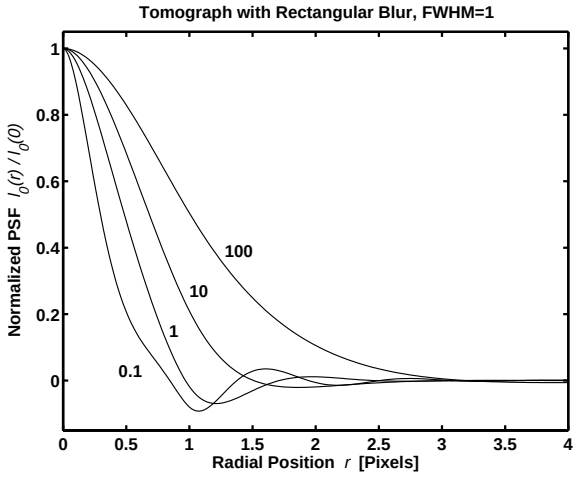

Figure 6: As in Fig. 5, but for a tomograph with a rectangular detector blur: $S_{\rm true}(u) = \mathrm{sinc}(u)$.

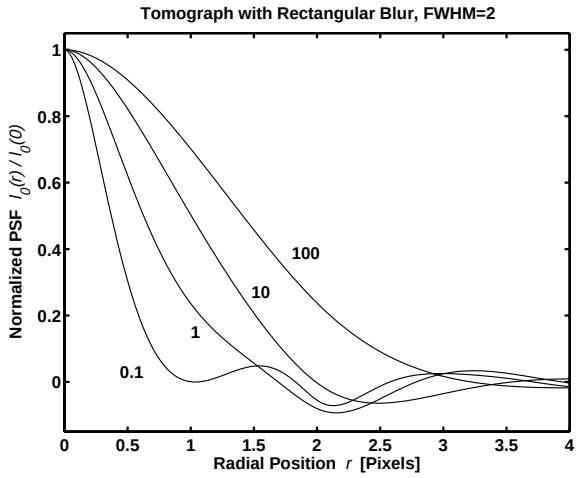

Figure 7: As in the previous figure, except $S_{\rm true}(u) = \mathrm{sinc}(2u)$.

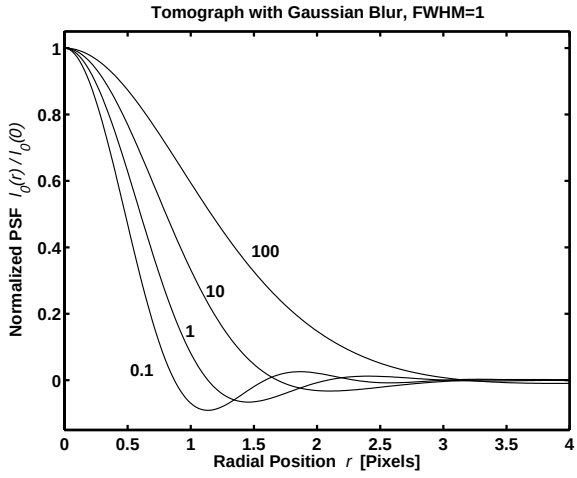

Figure 8: As in Fig. 5, but for a tomograph with a Gaussian detector blur: $S_{\rm true}(u) = \exp(-2\pi^2 u^2/\sigma^2)$.

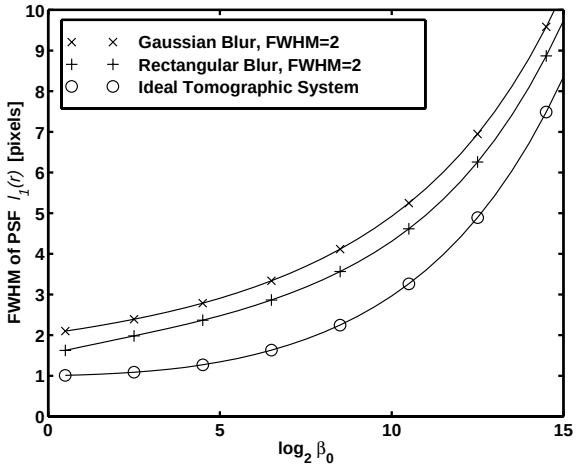

Figure 9: FWHM of the point spread functions $l_1(r)$ corresponding to the $l_0(r)$ shown in Figs. 5-8, as a function of the regularization parameter β_0.

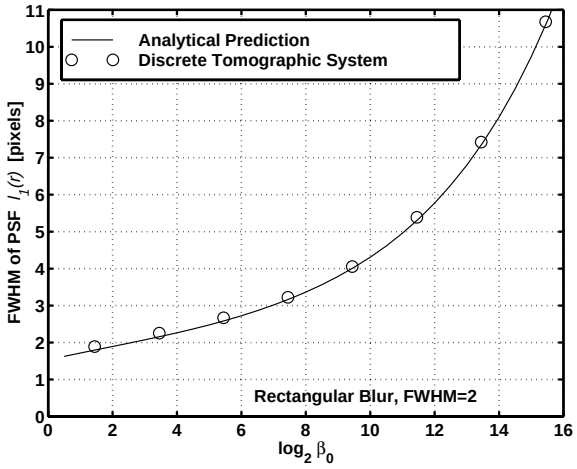

Figure 10: Comparison of the resolution of the analytically computed PSF (9) with the resolution of the discrete PSF ((38) of [1]), for a tomograph with rectangular blur: $S_{\rm true}(u) = \mathrm{sinc}(2u)$.

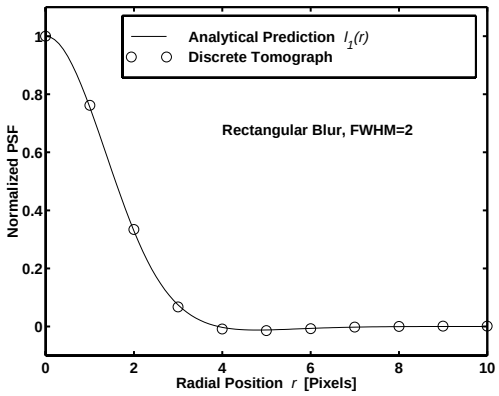

Figure 11: Comparison of analytically predicted PSF using (9) and discrete PSF from (38) of [1], for a tomograph with rectangular blur: $S_{\rm true}(u) = \mathrm{sinc}(2u)$.

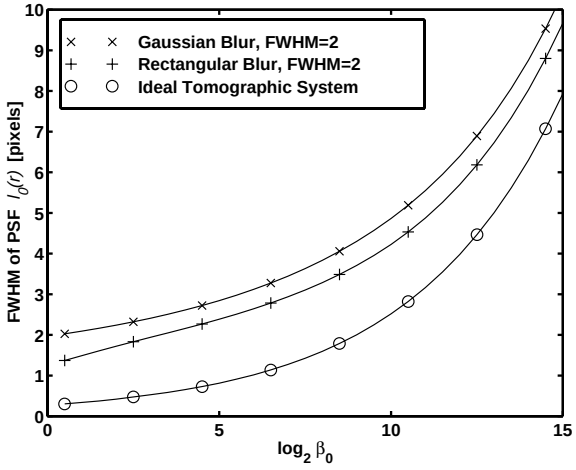

Figure 12: FWHM of $l_0(r)$ versus $\log_2(\beta_0)$, for various detector responses.

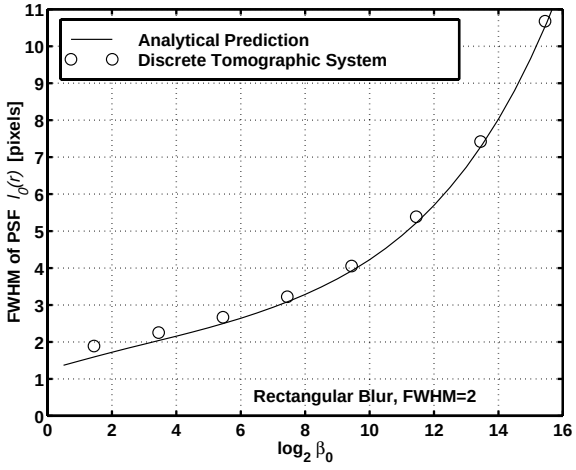

Figure 13: As in Fig. 10 but for $l_0(r)$.